# Estimating internuclear distances between half-integer quadrupolar nuclei by central-transition double-quantum sideband NMR spectroscopy

**Andreas Brinkmann and Mattias Edén**

Can. J. Chem. Downloaded from www.nrcresearchpress.com by National Research Council of Canada on 07/28/11
For personal use only.

**Abstract:** We demonstrate the estimation of homonuclear dipolar couplings, and thereby internuclear distances, between half-integer spin quadrupolar nuclei by central-transition (CT) double-quantum (2Q) sideband nuclear magnetic resonance (NMR) spectroscopy. It is shown that the rotor-encoded sideband amplitudes from CT 2Q coherences in the indirect dimension of the two-dimensional NMR spectrum are sensitive probes of the magnitude of the homonuclear dipolar coupling, but are significantly less affected by other NMR parameters such as the magnitudes and orientations of the electric field gradient tensors. Experimental results of employing the $R2_2^1R2_2^{-1}$ recoupling sequence to the $^{11}B$ spin pair of bis(catecholato)diboron resulted in an estimation of the internuclear B–B distance as (169.6 ± 3) pm, i.e., with a relative uncertainty of ±2%, and in excellent agreement with the distance of 167.8 pm determined by single-crystal X-ray diffraction.

*Key words:* solid-state NMR, quadrupolar nuclei, central transition, double-quantum coherence, sideband spectroscopy, distance estimation.

**Résumé :** Faisant appel à la spectroscopie de résonance magnétique nucléaire (RMN) à transition centrale (TC) avec une bande latérale à double quantum (2Q), on montre qu'il est possible d'évaluer les couplages dipolaires homonucléaires, et ainsi les distances internucléaires, entre des noyaux quadripolaires de spin une demie. On montre que les amplitudes des bandes latérales encodées par un rotor, obtenues à partir des cohérences de la TC 2Q dans la dimension indirecte de spectre RMN bidimensionnel, sont des sondes sensibles de l'amplitude de couplage dipolaire homonucléaire, mais qu'elles sont moins influencées par d'autres paramètres de la RMN, tel les amplitudes et les orientations des tenseurs du gradient du champ électrique. Les résultats expérimentaux obtenus en employant la séquence de recouplage $R2_2^1R2_2^{-1}$ à la paire de spin $^{11}B$ du bis(catécholato)dibore à permis de faire d'évaluer la distance internucléaire B–B à (169,6 ± 3) pm, c'est-à-dire avec une incertitude relative de ±2 %, et en excellent accord avec la distance de 167,8 pm déterminée par diffraction des rayons-X sur un cristal unique.

*Mots-clés :* RMN à l'état solide, noyau quadripolaire, transition centrale, cohérence à double quantum, spectroscopie des bandes latérales, évaluation de la distance.

[Traduit par la Rédaction]

## Introduction

The utilization of through-space dipolar interactions is of pivotal importance for determining order, structure, and dynamics by solid-state nuclear magnetic resonance (NMR) spectroscopy.[1–3] The anisotropic (orientation-dependent) dipolar interactions may provide both geometric and interatomic distance-related structural information; the latter feature stems from the inverse cubic relationship between the separation ($r_{jk}$) of two NMR-active nuclei and their dipolar coupling constant ($b_{jk}$). Solid-state NMR experimentation is generally performed on powdered samples undergoing magic-angle spinning (MAS) to emphasize isotropic (orientation-independent) nuclear spin interactions by reducing, or even eliminating, the anisotropies. However, during one or several segments of the MAS NMR experiment, the effects of the dipolar interactions may temporarily be reactivated: this process is referred to as "dipolar recoupling" and is typically arranged by application of radio-frequency (rf) pulse sequences.[1–3]

This work exploits "homonuclear" dipolar interactions (i.e., couplings involving nuclei of the same type) among half-integer spin quadrupolar nuclei[4–20] for estimating internuclear distances. Half-integer spins dominate among all existing NMR-active nuclei; examples include $^{11}B$, $^{17}O$, $^{23}Na$, $^{27}Al$, and $^{43}Ca$. Following the advent of high-resolution solid-state NMR techniques, to eliminate the broadening from second-order quadrupolar interactions of the central transitions

Received 1 November 2010. Accepted 25 January 2011. Published at www.nrcresearchpress.com/cjc on XX July 2011.

**A. Brinkmann.** Steacie Institute for Molecular Sciences, National Research Council, 1200 Montreal Road, M-40, Ottawa, ON K1A 0R6, Canada.
**M. Edén.** Physical Chemistry Division, Department of Materials and Environmental Chemistry, Arrhenius Laboratory, Stockholm University, 106 91 Stockholm, Sweden.

**Corresponding author:** Andreas Brinkmann (e-mail: Andreas.Brinkmann@nrc-cnrc.gc.ca).

*This article is part of a Special Issue dedicated to Professor Roderick E. Wasylishen.*



RIGHTSLINK

Can. J. Chem. Downloaded from www.nrcresearchpress.com by National Research Council of Canada on 07/28/11
For personal use only.

(CTs),[21–24] half-integer spins have become indispensable probes of local structure in widely diverse materials of technological and geological importance.[25–27]

An important subclass of recoupling methodology exploits dipolar interactions for generating double-quantum coherences (2QC) under MAS conditions.[2,3] Such recoupling techniques targeting the CTs of half-integer spins, i.e., employing rf fields that are weak compared with the quadrupolar frequency, have primarily been utilized in two-dimensional 2Q-1Q NMR correlation spectroscopy that reveals all pairs of spatially nearby homonuclear spins in the structure.[11,12,15,19] A double-quantum filtering (2QF) stage in a 2Q-1Q NMR experiment involves two events, one for creating 2QC from longitudinal magnetization and one for driving the reverse process.[2,3] Such "excitation" and "reconversion" intervals are often of equal duration: $\tau_{exc} = \tau_{rec}$ (Fig. 1*a*). They are interleaved by an evolution period ($t_1$), during which each 2QC acquires a phase factor involving the frequency sum of the two spin resonances within the pair. Each 2QC frequency, appearing along the indirect ($\omega_1$) dimension of the 2D spectrum, becomes correlated with its two respective CT single-quantum coherence (1QC) frequencies along the direct ($\omega_2$) spectral dimension.[11,12,15,19]

It is normally desirable to sample the $t_1$ evolution such that it is synchronized with the rotational period $\tau_r = 2\pi/\omega_r$ of the sample, where $\omega_r$ denotes the angular rotation frequency; then, all spinning sidebands fold onto the centre-band frequency. Besides improving signal-to-noise in the NMR spectrum and eliminating ambiguities in assigning the 2D NMR peaks, this avoids formation of intense sidebands along the 2QC dimension because of the orientation dependence of the (re)coupled dipolar Hamiltonian.[29–34] Such "rotor-encoded" spinning sidebands arise unless the 2QC excitation and reconversion processes are initiated at exactly the same rotor position. However, as the spinning-sideband amplitudes depend on the magnitudes of the anisotropic interaction tensors relative to the spinning frequency, they provide a vehicle to estimate dipolar coupling constants, and thereby internuclear distances, as introduced for spin-1/2 applications by Spiess and co-workers.[29–34] Here, we demonstrate the possibility of using such 2Q-1Q NMR correlation protocols for estimating internuclear distances between dipolar-coupled homonuclear half-integer spins. The dipolar recoupling and 2QC generation employed herein invokes symmetry-based pulse schemes,[3,35–41] as introduced by us for recoupling homonuclear quadrupolar spins,[15–17,19,42] under both MAS and double rotation (DOR)[21] conditions.

We present one of very few techniques for estimating homonuclear dipolar couplings among half-integer spin quadrupolar nuclei. Previous options include monitoring the 2QF signal buildup versus $\tau_{exc}$,[43] as is well-established for spin-1/2 applications,[2,3] or using magnetization transfers under a 2Q Hamiltonian[9,10] such as 2Q-HORROR.[35] In that case, one spectral dimension reveals a "Pake-like" pattern (whose width is proportional to $b_{jk}$) and may be implemented either as a 2D[10] or 3D[9] experiment, the latter incorporating triple-quantum MAS (3QMAS)[23] for improved NMR signal separation. Duer presented a strategy for homonuclear distance measurements by analyzing the spinning sideband formation originating from the evolution of triple-quantum coherences under homonuclear dipolar interactions in a 3QMAS experiment, coupled to multi-spin simulations based on the known crystal structure.[4] This approach did not invoke explicit dipolar recoupling but rather exploited spontaneous recoupling owing to the noncommutation of homonuclear dipolar and first-order quadrupolar interactions of half-integer spins.[4,8,44]

**Fig. 1.** (*a*) Radiofrequency pulse sequence to record two-dimensional homonuclear double-quantum correlation spectra on half-integer quadrupolar nuclei. The subscript "sel" indicates central-transition-selective pulses. A frequency sweep (FS) may be used to enhance the central transition population difference. The rotor-synchronized pulse sequence $R2_2^1R2_2^{-1}$ achieves homonuclear recoupling.[15] (*b*) Coherence transfer pathway diagram[28] for the *I* spins.

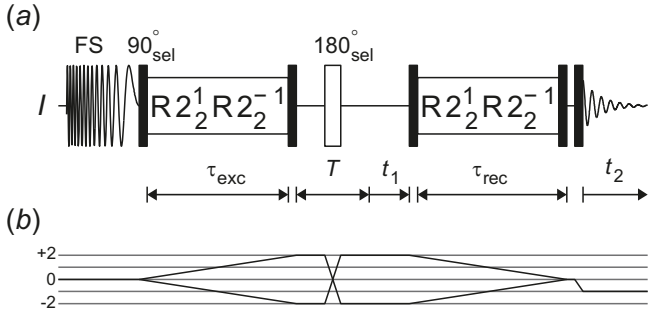


As isolated quadrupolar spin-pairs are rarely encountered, recoupling applications aiming at obtaining quantitative internuclear distances must generally consider large spin systems. To avoid such multi-spin effects and communicate the proof-of-principle, we here estimate the $^{11}B$–$^{11}B$ dipolar coupling and hence the internuclear B–B distance of the (isolated) pair of magnetically equivalent $^{11}B$ in the bis(catecholato)diboron molecule by 2Q-1Q correlation NMR spectroscopy. To support the analysis of the CT 2Q sideband NMR spectroscopy results, we calculated the $^{11}B$ chemical shift and quadrupolar tensors in bis(catecholato)diboron using gauge-including projector-augmented wave (GIPAW) density functional theory (DFT).[45] Our results are compared with those obtained by Weiss and Bryce[46] from various monoboronic acids and esters by DFT computations of isolated monomers and dimers.

## Materials and methods

### Solid-state NMR experiments

Figure 1 shows the pulse scheme used to obtain two-dimensional central-transition double-quantum (2D-CT-2Q) spectra of half-integer quadrupolar nuclei. At the start of the pulse sequence, the CT magnetization may optionally be enhanced;[13] possibilities include frequency sweeps as in Fig. 1*a*, encompassing double-frequency sweeps,[47] hyperbolic secant pulses,[48,49] and WURST single-frequency sweeps.[50] Other alternatives include the fast amplitude modulated (FAM)[51] and the equivalent rotor-assisted population transfer (RAPT) schemes,[52] or pulse shapes derived from optimal control theory.[53] The CT longitudinal magnetization is converted into homonuclear 2QC by a CT selective $R2_2^1R2_2^{-1}$ pulse sequence[15] of duration $\tau_{exc}$ that is bracketed by two CT 90° pulses; alternatively, for samples involving large spreads in resonance frequencies, it may be beneficial to employ the recoupling schemes of ref. 16. The 2QC are next subjected to a Hahn echo of total duration *T*,[15] adjusted so that the sum of



RIGHTSLINK

Can. J. Chem. Downloaded from www.nrcresearchpress.com by National Research Council of Canada on 07/28/11
For personal use only.

the CT 90° pulses and $T$ equals an even multiple of rotational periods (here, $2\tau_r$). The CT selective 180° refocusing pulse combined with phase cycling selects the coherence transfer pathway[28] shown in Fig. 1*b*.[12] After the subsequent evolution interval $t_1$, the 2QC are reconverted into longitudinal CT magnetization by a second $R2_2^1R2_2^{-1}$ block of duration $\tau_{rec}$, which is also sandwiched by CT 90° pulses. Finally, observable CT transverse magnetization is created by a CT selective 90° read pulse.

A powdered sample of bis(catecholato)diboron (molecular structure shown in Fig. 2) was purchased from Sigma-Aldrich and used for all experiments. The experimental results shown in Figs. 3–6 were obtained at a $^{11}$B Larmor frequency of –160.5 MHz in a static magnetic field of 11.75 T, by using a Bruker Advance-III console and a Varian 3.2 mm double-resonance standard-bore MAS probehead. The sample was rotated at a spinning frequency of 25 kHz, which corresponded to an rf nutation frequency of 6.25 kHz during dipolar recoupling, i.e., to a CT nutation frequency equal to half the MAS frequency,[15] as for the HORROR condition.[9,10,35] The selective 90° and 180° pulses operated at 9.0 kHz CT nutation frequency. All rf amplitudes were calibrated by complete 2D rf nutation experiments. To enhance the CT population difference, a single-frequency sweep was performed at the same rf field strength, by using a frequency offset and sweep bandwidths of 500 and 800 kHz, respectively, where the beginning and end of the sweep-pulse shape were attenuated by a $\sin^2$ and a $\cos^2$ function, respectively. The States-TPPI scheme was employed to obtain 2D pure absorption line shapes and to distinguish positive and negative 2Q coherences.[54,55]

### Numerical spin dynamics simulations

All $^{11}$B spin-pair simulations were performed using version 3.0.1 of the SIMPSON package.[56] The experimental parameters given in the preceding subsection were used, together with the experimentally estimated values of the $^{11}$B quadrupolar coupling constant and asymmetry parameter listed in Table 1. In addition, the parameters of the CSA tensor and the orientation of the quadrupolar tensor were employed as obtained by GIPAW-DFT calculations (see Table 1). For all cases, powder averaging was accomplished by using a set of triplets of Euler angles, selected according to the ZCW scheme.[57–59] This set consisted of 1154 angles for simulating the CT 2Q build-up curves shown in Fig. 3, whereas the calculations of the CT 2Q sideband patterns displayed in Figs. 5 and 6 employed 6044 orientations. All pulses were taken explicitly into account in the simulations, except for the CT population enhancement and the 90° read pulse. The initial density operator and the detection operator were both set to represent CT $z$-magnetization. The CT 2QC were selected by setting all other elements in the density matrix to zero before and after the 180° spin-echo pulse. The CT 2Q sideband amplitudes were simulated by incrementing $t_1$ in 35 steps of duration $\tau_r/35$ and combining the results of the +2QC and –2QC time-dependent signal amplitudes to form the cosine and sine components required by the States procedure.[54] The resulting complex $t_1$ time signal was subjected to a complex Fourier transformation to obtain the integrated CT 2Q spinning sideband amplitudes.

### Quantum chemical calculations

For the GIPAW-DFT calculations of the $^{11}$B quadrupolar and chemical shift tensors in bis(catecholato)diboron, CASTEP[60] and CASTEP-NMR[45,61,62] (version 4.4) were used together with Accelrys' Materials Studio. The generalized gradient approximation with the Perdew–Burke–Ernzerhof exchange correlation functional[63] and "on-the-fly" pseudopotentials were chosen. The plane-wave cutoff energy was selected to be 550 eV and the $k$-point grid was set to $5 \times 2 \times 4$. Starting from the structure determined by single-crystal X-ray diffraction (XRD),[64] initially, only the proton positions were optimized, whereupon the NMR parameters were calculated.

## Results and discussion

### $^{11}$B NMR parameters in bis(catecholato)diboron

To use the full set of $^{11}$B NMR parameters for bis(catecholato)diboron in the numerical simulations of the dipolar recoupling experiments, in a first step, we determined the $^{11}$B isotropic shift, quadrupolar coupling constant $C_Q = e^2qQ/h$ and the quadrupolar asymmetry parameter $\eta_Q$ experimentally; the results are shown in Table 1. In a second step, we derived the $^{11}$B quadrupolar and chemical shift tensors in bis(catecholato)diboron by GIPAW-DFT calculations. Weiss and Bryce[46] recently reported $^{11}$B NMR parameters in various monoboronic acids and esters by using DFT computations of isolated monomers and dimers. Since a crystal structure of bis(catecholato)diboron has been determined using single-crystal XRD,[64] we chose GIPAW-DFT calculations that explicitly account for the periodicity of the crystal.[45] The results of these computations are displayed in Table 1 and Fig. 2. Since the two boron sites in the bis(catecholato)diboron molecule are related by inversion symmetry through the centre of their internuclear vector, the chemical shift tensors, as well as quadrupolar tensors, are identical for both boron sites (magnitudes and orientations). The experimentally determined isotropic chemical shift and quadrupolar coupling constant of $\delta_{iso} = 28.6$ ppm and $C_Q = 2.71$ MHz, respectively, fall into the same range as that found for monoboronic esters,[46] whilst the present value $\eta_Q = 0.745$ is larger than those of the esters. Figure 2 shows the principle axis systems of the tensors, as obtained from GIPAW-DFT computations. The $z$ principal axes of both tensors are approximately perpendicular to the molecular plane and the $y$ axes are nearly collinear with the B–B bond. Whilst the calculated value $\eta_Q = 0.77$ is in good agreement with the experimentally determined one, the computed value $C_Q = 3.18$ MHz is significantly larger (by ≈0.5 MHz) than the experimentally measured value. In the Haeberlen notation[65] the calculated anisotropic chemical shift and asymmetry parameter are given by $(\delta_{aniso}, \eta) = (–22.6$ ppm, 0.67), which corresponds to a span and skew of $(\Omega, \kappa) = (41.5$ ppm, 0.27) in the Maryland notation.[65] We note that the calculated span is slightly higher than the largest one found in monoboronic acids,[46] whereas the skew is smaller.

### Central-transition double-quantum NMR spectroscopy

A common approach to determine homonuclear dipolar couplings is to monitor the buildup of 2QC as a function of the excitation interval $\tau_{exc}$ of the recoupling sequence. This approach was launched by Mali et al.[12] in the present context



RIGHTSLINK

**Table 1.** $^{11}$B NMR parameters of bis(catecholato)diboron as determined experimentally and by GIPAW-DFT calculations. The reported values of the anisotropic chemical shift ($\delta_{aniso}$) and the asymmetry parameter ($\eta$) conform to the Haeberlen notation.[60]

| | $C_Q$ (MHz) | $\eta_Q$ | $\Omega^Q_{PM}$ (°) | $\{\sigma_{xx}, \sigma_{yy}, \sigma_{zz}\}$ (ppm) | $\delta_{iso}$ (ppm) | $\delta_{aniso}$ (ppm) | $\eta$ | $\Omega^{CSA}_{PM}$ (°) |
|---|---|---|---|---|---|---|---|---|
| Exptl. | 2.71 | 0.745 | | | 28.6 | | | |
| DFT | 3.18 | 0.77 | {–87.7, 89.8, 179.9} | {48.2, 63.4, 89.7} | | –22.6 | 0.67 | {–87.3, 85.8, –178.6} |

**Note:** The Euler angles $\Omega^{\Lambda}_{PM}$ give the relative orientation of the principle axis system of the interaction tensor $\mathbf{\Lambda}$ and a molecule fixed frame with its $z$ axis along the B–B internuclear vector and its $x$ axis perpendicular to the O–B–O plane (compare Fig. 2). $C_Q$, quadrupolar coupling constant; $\eta_Q$, quadrupolar asymmetry parameter; $\{\sigma_{xx}, \sigma_{yy}, \sigma_{zz}\}$, principal components of the chemical shielding tensor; $\delta_{iso}$, isotropic chemical shift.

**Fig. 2.** Molecular structure of bis(catecholato)diboron.[64] The principal axis system of the $^{11}$B quadrupole coupling and chemical shift tensors as determined by CASTEP calculations are indicated in black and blue colors, respectively.

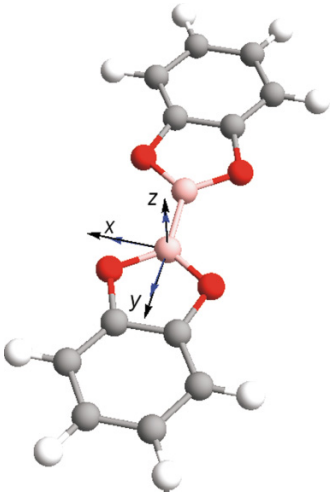


**Fig. 3.** $^{11}$B double-quantum filtered efficiencies as a function of $\tau_{exc} = \tau_{rec}$ obtained in bis(catecholato)diboron using the pulse sequence shown in Fig. 1 at a spinning frequency of 25 kHz and an external field of 11.75 T. Experimental results are indicated by ■, whereas the outcome of numerical simulations for different homonuclear dipolar couplings constants $b_{jk}/2\pi$ are displayed as –2619 Hz (●), –3119 Hz (▲), and –2119 Hz (▼).

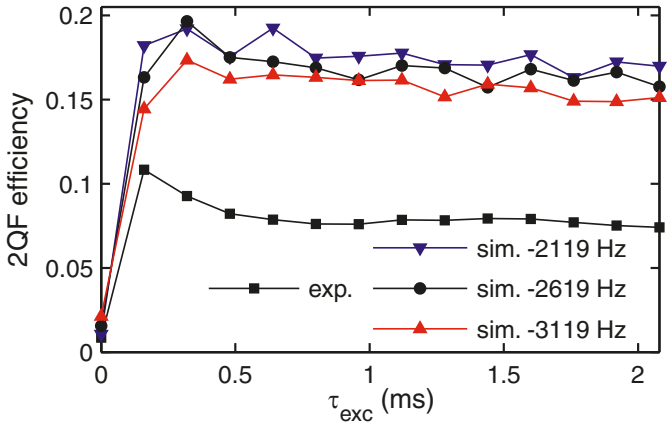


of distance estimations among half-integer spins. Figure 3 shows experimental and simulated $^{11}$B two-spin 2QF efficiencies as a function of $\tau_{exc} = \tau_{rec}$, as determined in bis(catecholato)diboron by using the pulse sequence shown in Fig. 1 at a spinning frequency of 25 kHz and an external field of 11.75 T. Single-crystal XRD provided the B–B internuclear distance $r_{jk}$ = 167.8 pm in the bis(catecholato)diboron molecule,[64] corresponding to a $^{11}$B–$^{11}$B coupling constant of $b_{jk}/2\pi$ = –2619 Hz. The numerically simulated results in Fig. 3 account for the $^{11}$B natural abundance of 80.1% that results in a probability of 64.2% to find a $^{11}$B–$^{11}$B spin pair in an arbitrarily selected molecule. We achieved an experimental 2QF efficiency of 11%, whereas the simulation employing a $^{11}$B–$^{11}$B dipolar coupling of –2619 Hz predicts a maximum 2QF efficiency of 20%. For comparison, Fig. 3 additionally displays the results of numerical simulations using dipolar couplings of –2119 and –3119 Hz. Minor variations of the $^{11}$B 2QC dynamics were observed, despite the large difference between the dipolar couplings, which makes this approach an unfavourable choice if accurate determinations of large homonuclear dipolar couplings are desired. Significantly faster sample rotation would allow for finer sampling of the 2QC buildup, however, at the expense of requiring higher rf field strengths during recoupling: this compromises the CT selectivity of the pulses, while also leading to higher accumulation of rf errors during the 2Q-recoupling events. For the present experimental conditions, the problem of too coarse sampling of $\tau_{exc}$ prevails even for estimates of smaller couplings ($b_{jk} \approx 0.5$ kHz) and is accentuated further for homonuclear systems involving higher spin numbers (e.g., $^{27}$Al) because of their accelerated 2QC excitation.[12,17]

Here we propose to instead utilize the spinning sidebands of the two-spin CT 2QC as a more favourable option for determining homonuclear dipolar couplings between half-integer quadrupolar nuclei. It offers particular advantages for measurements of strong dipolar interactions. In addition, whereas the efficiency of exciting CT 2QCs itself depends on the ability to employ CT-selective rf fields, the CT 2Q sideband patterns are significantly less influenced by this requirement. Although in the case of powdered samples, the rf fields may not be CT selective for all crystallite orientations at all time points, in practice this poses no serious limitation to the applicability of CT 2Q spectroscopy.[15–19]

Figure 4 shows the experimental $^{11}$B 2D CT 2Q spectra of bis(catecholato)diboron, obtained by using the pulse sequence in Fig. 1 for three different intervals $\tau_{exc} = \tau_{rec}$ of 160, 320, and 480 μs at a spinning frequency of 25 kHz. The NMR spectra comprise strong rotor-encoded odd-order spinning sidebands in the indirect (2Q) dimension, analogous to the cases of coupled spin-1/2 nuclei or isolated quadrupolar spins, described by the group of Spiess.[29–34] If $t_1$ is incremented by a fraction of the rotational period under relatively fast MAS conditions, these sidebands mainly result from rotor encoding of the 2Q reconversion process. The rotor-encoded modulation of the 2QC gives rise solely to *odd-ordered*

Can. J. Chem. Downloaded from www.nrcresearchpress.com by National Research Council of Canada on 07/28/11
For personal use only.



RIGHTSLINK

Can. J. Chem. Downloaded from www.nrcresearchpress.com by National Research Council of Canada on 07/28/11
For personal use only.

**Fig. 4.** Experimental two-dimensional $^{11}$B central-transition (CT) double-quantum (2Q) spectra of bis(catecholato)diboron for different time intervals $\tau_{exc} = \tau_{rec}$: (*a*) 160 μs, (*b*) 320 μs, and (*c*) 480 μs.

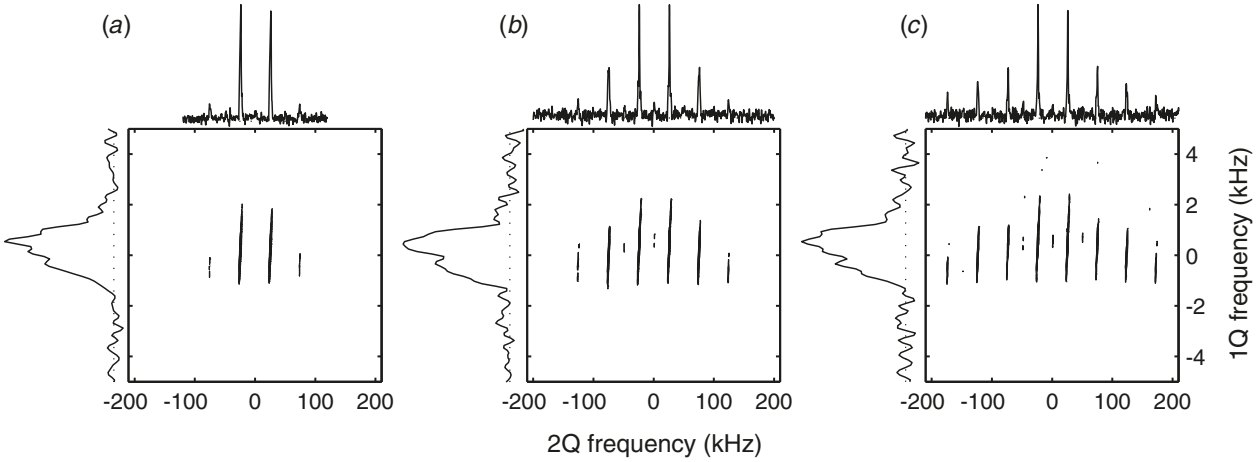


sidebands along the 2Q spectral dimension, even in scenarios devoid of 2QC evolution during $t_1$.[32,33] Ideally, the number and amplitudes of the sidebands depend only on the product $b_{jk}\tau_{rec}$ of the homonuclear dipolar coupling constant and the reconversion interval. On the other hand, the evolution of the 2QC under *all* noncommuting spin interactions during the $t_1$ interval produce conventional sidebands involving *all orders*, owing to the *rotor modulation* of the 2QC. The very small amplitudes of the even-order sidebands in the experimental spectra shown in Fig. 4 verify that hardly any rotor-modulated sidebands are present and that the rotor encoding of the 2Q reconversion process is indeed the predominant contribution to the odd-order sidebands. As expected,[29–34] a larger number of sidebands appear along the 2Q dimension of the 2D spectrum as the interval $\tau_{exc} = \tau_{rec}$ increases (Fig. 4).

The integrated amplitudes of the odd-ordered sidebands of the experimental $^{11}$B 2D CT 2Q spectra of bis(catecholato)diboron are plotted in Figs. 5*a*, 5*c*, and 5*e* against the sideband order. For comparison, results of numerical simulations using the XRD distance-based $^{11}$B–$^{11}$B dipolar coupling of $b_{jk}/2\pi = -2619$ Hz are presented in Figs. 5*b*, 5*d*, and 5*f*: the top row, (*a*) and (*b*), compares the experimental and simulated results for $\tau_{exc} = \tau_{rec} = 160$ μs; the middle row, (*c*) and (*d*), for 320 μs; and the bottom panel, (*e*) and (*f*), for 480 μs. It is evident that the experimental and simulated CT 2Q odd-order sideband amplitudes are similar overall, except from those of the ±1 sidebands that are more intense in the experiments relative to the simulations. However, the higher order (±3, ±5,…) sideband patterns are reproduced remarkably well. For internuclear distance measurements, we consequently suggest selecting $\tau_{exc} = \tau_{rec}$ sufficiently large, so that at least the ±3, ±5 and ±7 sidebands are present in the CT 2Q-1Q spectra.

To assess the sensitivity of the CT 2Q sideband pattern for the purpose of estimating the $^{11}$B–$^{11}$B dipolar coupling $b_{jk}$ and hence the B–B internuclear distance $r_{jk}$, we performed a series of numerical simulations for $\tau_{exc} = \tau_{rec} = 480$ μs by varying the dipolar coupling constants in steps of 20 Hz between –3619 and –1699 Hz. In each case we fitted one overall scaling factor of the complete sideband pattern by minimizing the sum-square deviation $S$ between the simulated and experimental (±3, ±5, ±7, ±9) integrated sideband amplitudes. The 95% confidence interval was determined by the set of dipolar couplings for which $S \leq S_{min}\{1 + F^{0.05}_{1,6}/6\}$, where $S_{min}$ is the sum-square deviation for the best fit and $F^{\alpha}(p_1,p_2)$ is the upper $\alpha$ probability point of the $F$ distribution with $p_1$ and $p_2$ degrees of freedom.[66,67] We obtained a best fit

**Fig. 5.** Integrated odd-order CT 2Q spinning sideband amplitudes obtained in bis(catecholato)diboron for different time intervals $\tau_{exc} = \tau_{rec}$: (*a*) and (*b*) 160 μs, (*c*) and (*d*) 320 μs, and (*e*) and (*f*) 480 μs. The left column (*a*), (*c*), and (*e*) show experimental integrals, whereas the right column (*b*), (*d*), and (*f*) display numerically simulated sideband amplitudes for an $^{11}$B–$^{11}$B dipolar coupling of $b_{jk}/2\pi = -2619$ Hz, which corresponds to an internuclear distance of 167.8 pm provided by single-crystal XRD.[64]

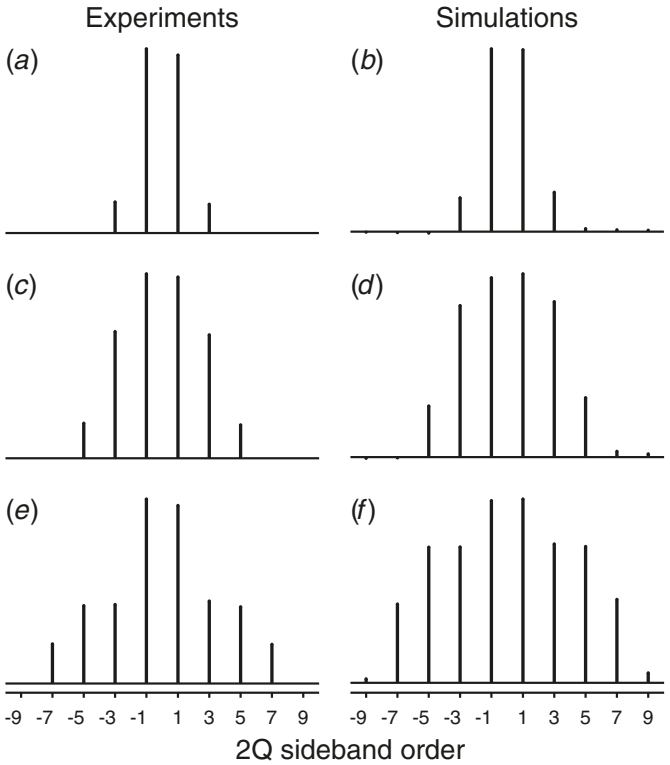




RIGHTSLINK

Can. J. Chem. Downloaded from www.nrcresearchpress.com by National Research Council of Canada on 07/28/11
For personal use only.

**Fig. 6.** Odd-order central-transition (CT) double-quantum (2Q) spinning sideband amplitudes obtained in bis(catecholato)diboron for $\tau_{exc} = \tau_{rec} = 480$ μs. Left column (*a*), (*c*), and (*e*): Blue/grey sticks depict the experimental integrals. Black sticks represent numerically simulated sideband amplitudes for different $^{11}B$–$^{11}B$ dipolar coupling constants $b_{jk}/2\pi$: (*a*) –2439 Hz, (*c*) –2579 Hz, and (*e*) –2699 Hz. Right column (*b*), (*d*), and (*f*): Simulated sideband amplitudes for $b_{jk}/2\pi = -2619$ Hz and different quadrupolar coupling constants $C_Q$: (*b*) 2.7 MHz, (*d*) 2.1 MHz, and (*f*) 3.5 MHz.

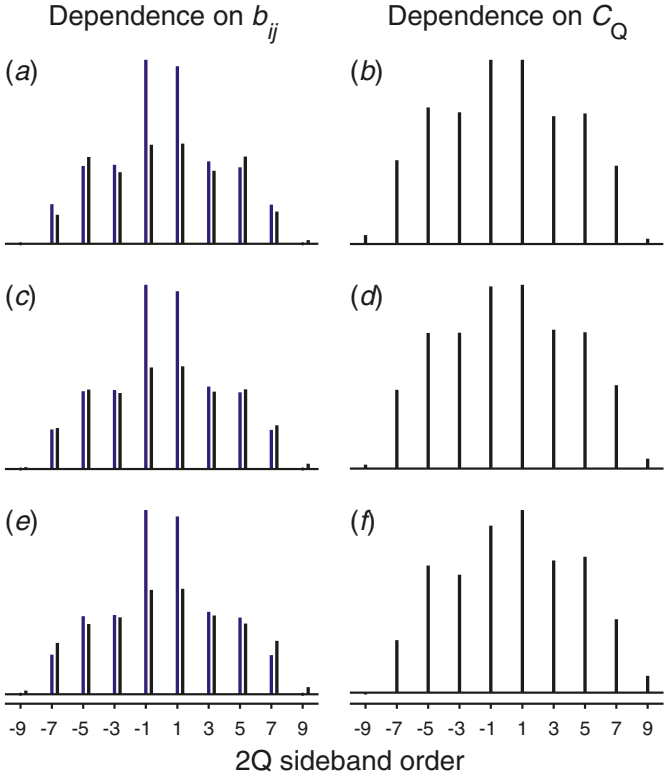


of –2579 (+70, –60) Hz for the $^{11}B$–$^{11}B$ dipolar coupling constant in bis(catecholato)diboron, which corresponds to a solid-state NMR-determined distance of 169.6 (+1.6, –1.3) ppm. These results are in excellent agreement with the values determined by X-ray diffraction, –2619 Hz and 167.8 pm, respectively. The best fit simulations of the CT 2Q sideband amplitudes are shown in Fig. 6*c* together with the experimental results.

In the right column of Fig. 6, the numerically simulated results from varying the quadrupolar coupling constant reveal very weak effects on the sideband amplitudes. This also applies if the quadruplar coupling constants of the two $^{11}B$ sites are different. Further, omitting the CSA interactions has even less bearing on the sideband patterns (data not shown). Numerical simulations (to be presented elsewhere) indicate that the quadrupolar coupling orientations, as well as the magnitude and orientation of the CSA tensor, only have relatively minor influences on the CT 2Q sideband pattern. However, because of these small effects, we conservatively state a final confidence interval for the estimation of the $^{11}B$–$^{11}B$ dipolar coupling constant in bis(catecholato)diboron that is twice the one found by the least-squares analysis. Therefore, we could reliably estimate the $^{11}B$–$^{11}B$ dipolar coupling constant as –2579 (+140, –120) Hz, corresponding to a solid-state NMR determined B–B distance of (169.6 ± 3) pm. Figures 6*a* and 6*e* show the experimental integrated CT 2Q sideband amplitudes together with the numerical simulations for the upper and lower bounds in the estimated dipolar coupling constant, i.e., –2439 and –2699 Hz, respectively. This confirms that the higher order (±3, ±5, …) sideband amplitudes clearly constitute sensitive measures of the homonuclear dipolar coupling. The relative uncertainty of our estimation is about ±5% in the $^{11}B$–$^{11}B$ dipolar coupling constant and about ±2% in the internuclear B–B distance.

Wi et al.[9,10] reported a recoupling-derived interatomic distance in the related bis(pinacolato)diboron complex, which also features two directly bonded boron atoms. Their approach utilized magnetization transfers under a 2Q dipolar Hamiltonian effected by the 2Q-HORROR technique[35] in the absence of 2QF. At the expense of significantly reduced NMR signal-to-noise, the explicit 2QF employed herein is advantageous for spin pairs where the recoupled isotope is not 100% naturally abundant (e.g., $^{11}B$), as it ensures that only one pair of the targeted spins need to be considered in the numerical simulations involved in the distance analysis. Similar issues apply for Duer's 3QMAS-based strategy.[4] Besides this favorable feature of the present technique, we expect that its accuracy and resolution of the distance estimates provided will be at least as good as the methods presented in refs. 4, 10, and 43.

## Concluding remarks

In this contribution, we have demonstrated that CT 2Q sideband NMR spectroscopy has great potential for estimating the internuclear distances between half-integer spin quadrupolar nuclei. We showed that for the $^{11}B$ spin pair of bis(catecholato)diboron, the amplitudes of higher odd-order (±3, ±5,…) double-quantum rotor-encoded spinning sidebands could be reproduced very well by numerical simulations and constitute sensitive probes of the homonuclear $^{11}B$–$^{11}B$ dipolar interaction. This resulted in an estimation of the $^{11}B$–$^{11}B$ dipolar coupling constant in bis(catecholato)diboron to –2579 (+140, –120) Hz (approx. ±5%), corresponding to an internuclear solid-state NMR-determined B–B distance of (169.6 ± 3) pm (approx. ±2%). This value is in excellent agreement with the single-crystal XRD-determined distance of 167.8 pm.[64] Our estimation of the uncertainties is conservative and takes into account that the exact size and orientation of the quadrupolar tensor has a weak influence on the CT 2Q sideband amplitudes. As a result, our approach is directly applicable for readily distinguishing between scenarios involving (for instance) single or double-bonded B–B motifs.[68]

Whereas the present work has provided one of very few examples of internuclear distance measurements in pairs of *directly* bonded quadrupolar spin-3/2 nuclei,[9,10] this approach is neither limited to strong dipolar couplings nor spin-3/2 systems. In a forthcoming publication we will present analytical expressions facilitating the 2Q spinning-sideband analysis and demonstrate the determination of much weaker homonuclear dipolar couplings among quadrupolar nuclei, such as $^{23}Na$ and $^{27}Al$, in the more commonly encountered context of inorganic network materials. Further, extensions of this work for determining heteronuclear dipolar interactions



RIGHTSLINK

involving half-integer quadrupolar nuclei[34,69,70] are in progress in our laboratories.

## Acknowledgments

The authors would like to thank G. Enright for confirming the X-ray structure of bis(catecholato)diboron and I. Moudrakovski, V. Terskikh, and C. Ratcliffe for helpful discussions. Access to CASTEP was provided by the National Ultrahigh-Field NMR Facility for Solids (Ottawa, Ontario), a national research facility funded by the Canada Foundation for Innovation, the Ontario Innovation Trust, Recherche Québec, the National Research Council Canada (NRC), and Bruker BioSpin and managed by the University of Ottawa (www.nmr900.ca). This work was supported by the National Research Council Canada, the Swedish Research Council (VR; contracts 2007-4967 and 2009-7551), and the Faculty of Natural Sciences at Stockholm University.

## References

(1) Bennett, A. E.; Griffin, R. G.; Vega, S. In *NMR Basic Principles and Progress;* Diehl, P., Fluck, E., Gunther, H., Kosfield, R., Seelig, J., Eds.; Springer-Verlag: Berlin, 1994; pp 1–77.

(2) Dusold, S.; Sebald, A. *Ann. Rep. NMR Spectrosc.* **2000** *41*, 185. doi:10.1016/S0066-4103(00)41010-0.

(3) Levitt, M. H. Symmetry-Based Pulse Sequences in Magic-Angle Spinning Solid-State NMR. In *Encyclopedia of Nuclear Magnetic Resonance;* Grant, D. M., Harris, R. K., Eds.; Wiley: Chichester, UK, 2002; Vol. 9, pp 165–196.

(4) Duer, M. J. *Chem. Phys. Lett.* **1997** *277* (1–3), 167. doi:10.1016/S0009-2614(97)00929-9.

(5) Baldus, M.; Rovnyak, D.; Griffin, R. G. *J. Chem. Phys.* **2000** *112* (13), 5902. doi:10.1063/1.481187.

(6) Dowell, N. G.; Ashbrook, S. E.; McManus, J.; Wimperis, S. *J. Am. Chem. Soc.* **2001** *123* (33), 8135. doi:10.1021/ja010681d.

(7) Edén, M.; Grinshtein, J.; Frydman, L. *J. Am. Chem. Soc.* **2002** *124* (33), 9708. doi:10.1021/ja020534v.

(8) Edén, M.; Frydman, L. *J. Phys. Chem. B* **2003** *107* (51), 14598. doi:10.1021/jp035794t.

(9) Wi, S.; Heise, H.; Pines, A. *J. Am. Chem. Soc.* **2002** *124* (36), 10652. doi:10.1021/ja027043v.

(10) Wi, S.; Logan, J. W.; Sakellariou, D.; Walls, J. D.; Pines, A. *J. Chem. Phys.* **2002** *117* (15), 7024. doi:10.1063/1.1506907.

(11) Painter, A. J.; Duer, M. J. *J. Chem. Phys.* **2002** *116* (2), 710. doi:10.1063/1.1425831.

(12) Mali, G.; Fink, G.; Taulelle, F. *J. Chem. Phys.* **2004** *120* (6), 2835. doi:10.1063/1.1638741.

(13) Mali, G.; Kaučič, V. *J. Magn. Reson.* **2004** *171* (1), 48. doi:10.1016/j.jmr.2004.08.003.

(14) Edén, M.; Annersten, H.; Zazzi, Å. *Chem. Phys. Lett.* **2005** *410* (1–3), 24. doi:10.1016/j.cplett.2005.04.030.

(15) Edén, M.; Zhou, D.; Yu, J. *Chem. Phys. Lett.* **2006** *431* (4–6), 397. doi:10.1016/j.cplett.2006.09.081.

(16) Lo, A. Y. H.; Edén, M. *Phys. Chem. Chem. Phys.* **2008** *10* (44), 6635. doi:10.1039/b808295b.

(17) Brinkmann, A.; Kentgens, A. P. M.; Anupõld, T.; Samoson, A. *J. Chem. Phys.* **2008** *129* (17), 174507. doi:10.1063/1.3005395.

(18) Edén, M.; Lo, A. Y. H. *J. Magn. Reson.* **2009** *200* (2), 267. doi:10.1016/j.jmr.2009.07.007.

(19) Edén, M. *Solid State NMR* **2009** *36* (1), 1. doi:10.1016/j.ssnmr.2009.06.005.

(20) Wang, Q.; Hu, B.; Lafon, O.; Trébosc, J.; Deng, F.; Amoureux, J. P. *J. Magn. Reson.* **2009** *200* (2), 251. doi:10.1016/j.jmr.2009.07.009.

(21) Samoson, A.; Lippmaa, E.; Pines, A. *Mol. Phys.* **1988** *65* (4), 1013. doi:10.1080/00268978800101571.

(22) Mueller, K. T.; Sun, B. Q.; Chingas, G. C.; Zwanziger, J. W.; Terao, T.; Pines, A. *J. Magn. Reson.* **1990** *86*, 470.

(23) Frydman, L.; Harwood, J. S. *J. Am. Chem. Soc.* **1995** *117* (19), 5367. doi:10.1021/ja00124a023.

(24) Gan, Z. *J. Am. Chem. Soc.* **2000** *122* (13), 3242. doi:10.1021/ja9939791.

(25) Smith, M. E.; van Eck, E. R. H. *Prog. Nucl. Magn. Reson. Spectrosc.* **1999** *34* (2), 159. doi:10.1016/S0079-6565(98)00028-4.

(26) Ashbrook, S. E.; Duer, M. J. *Concepts Magn. Reson. A* **2006** *28*, 183. doi:10.1002/cmr.a.20053.

(27) Hanna, J. V.; Smith, M. E. *Solid State NMR* **2010** *38* (1), 1. doi:10.1016/j.ssnmr.2010.05.004.

(28) Bodenhausen, G.; Kogler, H.; Ernst, R. R. *J. Magn. Reson.* **1984** *58*, 370.

(29) Geen, H.; Titman, J. J.; Gottwald, J.; Spiess, H. W. *J. Magn. Reson. A* **1995** *114* (2), 264. doi:10.1006/jmra.1995.1137.

(30) Gottwald, J.; Demco, D. E.; Graf, R.; Spiess, H. W. *Chem. Phys. Lett.* **1995** *243* (3–4), 314. doi:10.1016/0009-2614(95)00872-2.

(31) Graf, R.; Demco, D. E.; Gottwald, J.; Hafner, S.; Spiess, H. W. *J. Chem. Phys.* **1997** *106* (3), 885. doi:10.1063/1.473169.

(32) Friedrich, U.; Schnell, I.; Brown, S. P.; Lupulescu, A.; Demco, D. E.; Spiess, H. W. *Mol. Phys.* **1998** *95* (6), 1209. doi:10.1080/00268979809483252.

(33) Schnell, I.; Spiess, H. W. *J. Magn. Reson.* **2001** *151* (2), 153. doi:10.1006/jmre.2001.2336.

(34) Lupulescu, A.; Brown, S. P.; Spiess, H. W. *J. Magn. Reson.* **2002** *154* (1), 101. doi:10.1006/jmre.2001.2464.

(35) Nielsen, N. C.; Bildsøe, H.; Jakobsen, H. J.; Levitt, M. H. *J. Chem. Phys.* **1994** *101* (3), 1805. doi:10.1063/1.467759.

(36) Lee, Y. K.; Kurur, N. D.; Helmle, M.; Johannessen, O. G.; Nielsen, N. C.; Levitt, M. H. *Chem. Phys. Lett.* **1995** *242* (3), 304. doi:10.1016/0009-2614(95)00741-L.

(37) Edén, M.; Levitt, M. H. *J. Chem. Phys.* **1999** *111* (4), 1511. doi:10.1063/1.479410.

(38) Brinkmann, A.; Edén, M.; Levitt, M. H. *J. Chem. Phys.* **2000** *112* (19), 8539. doi:10.1063/1.481458.

(39) Carravetta, M.; Edén, M.; Zhao, X.; Brinkmann, A.; Levitt, M. H. *Chem. Phys. Lett.* **2000** *321* (3–4), 205. doi:10.1016/S0009-2614(00)00340-7.

(40) Brinkmann, A.; Levitt, M. H. *J. Chem. Phys.* **2001** *115* (1), 357. doi:10.1063/1.1377031.

(41) Brinkmann, A.; Edén, M. *J. Chem. Phys.* **2004** *120* (24), 11726. doi:10.1063/1.1738102.

(42) Edén, M. *J. Magn. Reson.* **2010** *204* (1), 99. doi:10.1016/j.jmr.2010.02.007.

(43) Mali, G.; Kaučič, V.; Taulelle, F. *J. Chem. Phys.* **2008** *128* (20), 204503. doi:10.1063/1.2928809.

(44) Edén, M.; Frydman, L. *J. Chem. Phys.* **2001** *114* (9), 4116. doi:10.1063/1.1344886.

(45) Pickard, C. J.; Mauri, F. *Phys. Rev. B* **2001** *63* (24), 245101. doi:10.1103/PhysRevB.63.245101.

(46) Weiss, J. W. E.; Bryce, D. L. *J. Phys. Chem. A* **2010** *114* (15), 5119. doi:10.1021/jp101416k.

(47) Kentgens, A. P. M.; Verhagen, R. *Chem. Phys. Lett.* **1999** *300* (3–4), 435. doi:10.1016/S0009-2614(98)01402-X.

(48) Siegel, R.; Nakashima, T. T.; Wasylishen, R. E. *Chem. Phys. Lett.* **2004** *388* (4–6), 441. doi:10.1016/j.cplett.2004.03.047.

Can. J. Chem. Downloaded from www.nrcresearchpress.com by National Research Council of Canada on 07/28/11
For personal use only.



RIGHTSLINK

(49) Siegel, R.; Nakashima, T. T.; Wasylishen, R. E. *J. Magn. Reson.* **2007** *184* (1), 85. doi:10.1016/j.jmr.2006.09.007.
(50) Hansen, M. R.; Brorson, M.; Bildsøe, H.; Skibsted, J.; Jakobsen, H. J. *J. Magn. Reson.* **2008** *190* (2), 316. doi:10.1016/j.jmr.2007.11.014.
(51) Madhu, P. K.; Goldbourt, A.; Frydman, L.; Vega, S. *J. Chem. Phys.* **2000** *112* (5), 2377. doi:10.1063/1.480804.
(52) Yao, Z.; Kwak, H.-T.; Sakellariou, D.; Emsley, L.; Grandinetti, P. J. *Chem. Phys. Lett.* **2000** *327* (1–2), 85. doi:10.1016/S0009-2614(00)00805-8.
(53) O'Dell, L. A.; Harris, K. J.; Schurko, R. W. *J. Magn. Reson.* **2010** *203* (1), 156. doi:10.1016/j.jmr.2009.12.016.
(54) States, D.; Haberkorn, R. A.; Ruben, D. J. *J. Magn. Reson.* **1982** *48*, 286.
(55) Marion, D.; Ikura, M.; Tschudin, R.; Bax, A. *J. Magn. Reson.* **1989** *85*, 393.
(56) Bak, M.; Nielsen, N. C. *J. Magn. Reson.* **2000** *147* (2), 296. doi:10.1006/jmre.2000.2179.
(57) Zaremba, S. K. *SIAM Rev.* **1968** *10* (3), 303. doi:10.1137/1010056.
(58) Conroy, H. *J. Chem. Phys.* **1967** *47* (12), 5307. doi:10.1063/1.1701795.
(59) Cheng, V. B.; Suzukawa, Jr., H. H.; Wolfsberg, M. *J. Chem. Phys.* **1973** *59* (8), 3992. doi:10.1063/1.1680590.
(60) Clark, S. J.; Segall, M. D.; Pickard, C. J.; Hasnip, P. J.; Probert, M. I. J.; Refson, K.; Payne, M. C. *Z. Kristallogr.* **2005** *220* (5–6), 567. doi:10.1524/zkri.220.5.567.65075.
(61) Yates, J. R.; Pickard, C. J.; Mauri, F. *Phys. Rev. B* **2007** *76* (2), 024401. doi:10.1103/PhysRevB.76.024401.
(62) Profeta, M.; Mauri, F.; Pickard, C. J. *J. Am. Chem. Soc.* **2003** *125* (2), 541. doi:10.1021/ja027124r.
(63) Perdew, J. P.; Burke, K.; Ernzerhof, M. *Phys. Rev. Lett.* **1996** *77* (18), 3865. doi:10.1103/PhysRevLett.77.3865.
(64) Clegg, W.; Elsegood, M. R. J.; Lawlor, F. J.; Norman, N. C.; Pickett, N. L.; Robins, E. G.; Scott, A. J.; Nguyen, P.; Taylor, N. J.; Marder, T. B. *Inorg. Chem.* **1998** *37* (20), 5289. doi:10.1021/ic9804317.
(65) Harris, R. K.; Becker, E. D.; Cabral de Menezes, S. M.; Granger, P.; Hoffman, R. E.; Zilm, K. W. *Pure Appl. Chem.* **2008** *80* (1), 59. doi:10.1351/pac200880010059.
(66) Seber, G. A. F.; Wild, C. J. *Nonlinear Regression;* Wiley Series in Probability and Statistics; Wiley-Interscience: Hoboken, NJ, 2003.
(67) Beale, E. M. L. *J. R. Stat. Soc., B* **1960** *22*, 41.
(68) Wang, Y.; Quillian, B.; Wei, P.; Wannere, C. S.; Xie, Y.; King, R. B.; Schaefer, H. F., III; von Ragué Schleyer, P.; Robinson, G. H. *J. Am. Chem. Soc.* **2007** *129* (41), 12412. doi:10.1021/ja075932i.
(69) Brinkmann, A.; Kentgens, A. P. M. *J. Phys. Chem. B* **2006** *110* (32), 16089. doi:10.1021/jp062809p.
(70) Brinkmann, A.; Kentgens, A. P. M. *J. Am. Chem. Soc.* **2006** *128* (46), 14758. doi:10.1021/ja065415k.

Can. J. Chem. Downloaded from www.nrcresearchpress.com by National Research Council of Canada on 07/28/11
For personal use only.



RIGHTSLINK